

Effect of MgO Addition on the Properties of Ni/Al₂O₃ and Its Catalytic Activity in Hydrogenation of N-(2',3'-dimethoxy benzyl)-3,4-dioxy-methylene-phenylethylamine

Guosheng Wang*, Xinxin Zhao and Siyu Han

Dept. of Chem. Eng., Shenyang university of chemical technology, 110041, China.

Wgsh-lyc@163.com*

(Received on 27th March 2018, accepted in revised form 31st January 2019)

Summary: the nickel based alumina-supported catalysts modified or promoted by magnesia were prepared by wet impregnation and successfully used for hydrogenation of N-(2',3'-dimethoxy benzyl)-3,4-dioxy-methylene-phenylethylamine, the 20Ni-6MgO/74Al₂O₃ samples exhibits the highest BET surface area, the largest pore volume, and the largest pore diameter in all of the samples such as Ni/Al₂O₃ and 20Ni-xMgO(80-x)Al₂O₃ excepted the highest BET surface area of Ni/Al₂O₃, the average pore diameter of the 20Ni-6MgO/74Al₂O₃ samples were two times as large as Ni/Al₂O₃, it was indicated that the function of expanding role or the mesoporosity was increased by addition of MgO, and MgO might be regarded as pore-enlarge agent for the bare Al₂O₃ support and benefit for the transport of large molecules reactants and products. The weak formation of MgO-Al₂O₃ and MgO-NiO solid solution as a result of competing interaction of MgO with Al₂O₃ support and NiO precursors restrained the strong interaction of NiO species with Al₂O₃ support, which favored the dispersion of active Ni centers and improved the reducible degree of NiO species on the surface of the catalysts. The improvement of basicity or the decrease in the number of acid centers in the catalysts avoid the secondary reactions, and subsequently resulted in high catalytic activity. The utilization of meso-porous 20Ni-6MgO/74Al₂O₃ for catalytic hydrogenation of N-(2',3'-dimethoxy benzyl)-3,4-dioxy-methylene-phenylethylamine (Shiff's base) with the highest selectivity of 99.70% and yields of 94.36% implied that the instead of Raney Ni was feasible.

Key Words: Ni/Al₂O₃, magnesia, hydrogenation, mesoporosity, competing interaction.

Introduction

Raney nickel catalysts were widely used for much more chemical process, such as (de)hydrogenation, hydrodesulfurization, and others, as a result of simply preparation, good thermal conductivity, high catalytic activity, and strong stability as a hydrogenation catalysts, it have been successfully applied to the chemical process such as hydrogenation of carbonyl, carboxyl, carbon-nitrogen bond, carbon-oxygen bond et. al., by now, Raney nickel was still used as catalysts for hydrogenation of N-(2',3'-dimethoxy benzyl)-3,4-dioxy-methylene-phenylethylamine, which was raw materials or intermediates for synthesis of berberine.

The supported nickel catalysts had been used for a wide variety of reactions, such as biomass conversion [1-5], (de)hydrogenation [6,7], partial oxidation [8, 9], steam reformation of methane [10-14], alcohol [15-18], and acetic acid [19], hydrodesulfurization [20], hydrogenolysis [21], decomposition [22] and others [23-25], to improve the selectivity, the heat stability, and the age of catalysts. The utilization of support nickel catalysts instead of Raney nickel was also a commonly strategy in production of chemical intermediates and pharmaceuticals.

The catalytic properties of supported metal catalysts depended mainly upon the specific atomic configuration, the number of atoms within a metal cluster and their interactions with the support surfaces become important in determining their catalytic performance [26-29]. When metal clusters are dispersed onto the high-surface-area supports, their interactions with the support surfaces may play a paramount role in determining their catalytic properties, subnanometer-sized metal clusters can have catalytic activity and /or selectivity different from sometimes better than ,their lager nanoparticles counterparts.

The nickel based alumina-supported catalysts modified or promoted by magnesia had aroused many researcher's interests [1, 2, 5-8, 15-18, 22, 24, 31], The introduction of MgO into the nickel based alumina-supported catalysts rebuild a synergy of three parties among Ni, Mg, and Al oxides, the interaction of Ni on the basic sites of the MgO(100) surface has been investigated using cluster models [32, 33], a moderately large interaction was predicted for interaction above the basic sites. the significantly stronger interaction of nickel oxide with Al₂O₃ than

*To whom all correspondence should be addressed.

with MgO, the dispersion of Ni was relatively poor on MgO [6], the strength of H-Ni bond was weakened on Ni/MgO was an important reason for the lowered activity of Ni/MgO for the hydrogenation of basic molecules, and the aromatic ring involved in the adsorption, the acidic support and electron-deficient Ni surface favored the adsorption of a aromatic ring. the Al ions can be well incorporated into the MgO lattice to form uniform Mg-Al oxides with small particle size of Ni nanoparticles [11]. The formation of new species not only adjust the surface acid-basic properties and ensures the high dispersion of nickel oxide, The presence of MgO reduces the number of acid centers corresponding to high values of ammonia adsorption energy [31]. a low calcination temperature (400°C) promoted the formation of small NiO species and reducible β -type NiO species, and a small addition of MgO could improved the catalysts stability, the spinel oxide NiAl_2O_4 formed at 400-450°C, and the NiMgO_2 solid solution formed at 500°C, [24]. an introduction of magnesium led to the formation of smaller nickel crystallites with stronger adsorption sites [22].the presence of MgO hindering the reduction of the NiO species in the catalysis helps to retain a high dispersion and finite the size of Ni particles, and a high Al content favored the strong basic site of the catalysts because of the synergistic effects among the components [8].

In the present work, the nickel based alumina-supported catalysts modified or promoted by magnesia were prepared by wet impregnation and used for the hydrogenation of N-(2',3'-dimethoxy benzyl)-3,4-dioxy-methylene-phenylethylamine, This paper mainly to solve the instead of Raney nickel by support nickel catalysts, the effect of MgO on the structure properties, the reducibility, and the interaction of the Ni-Mg-Al oxides in the catalysts.

Experimental

(1)Preparation of Catalysts

The catalysts were prepared by the wet impregnation method, The commercial Al_2O_3 particles were calcined at 500°C for 2h to increase pore volume and surface area, and then the Al_2O_3 particles were impregnated with an aqueous solution of $\text{Mg}(\text{NO}_3)_2 \cdot 6\text{H}_2\text{O}$ and $\text{Ni}(\text{NO}_3)_2 \cdot 6\text{H}_2\text{O}$ at room temperature for 24h, evaporated at 60°C, dried at 120°C for 3h, the mixture were sieved 200 mesh after tableting, crushing and grinding to keep the homogeneity, the precursor of the catalysts were prepared when the samples were calcined at 500°C for

5h, sieved 200 mesh after tableting, crushing and grinding again. The calcined samples was then reduced in hydrogen (H_2/Ar) with a flow rate of 50ml.min⁻¹, held at 500°C for 3h, and then cooled to the room temperature in argon atmosphere for experiments or further characterization. The different amount of MgO on the catalysts were loaded by changing the concentration of $\text{Mg}(\text{NO}_3)_2 \cdot 6\text{H}_2\text{O}$ of aqueous solution in the procedure of impregnation, the loading amount of Ni was 20 wt%, whereas the loading amount of MgO was varied ($x=0, 2, 4, 6, 8$ wt%), and Al_2O_3 varied (80,78,76,74,72wt%), respectively, the catalysts were denoted as $20\text{Ni-xMgO}/(80-x)\text{Al}_2\text{O}_3$, the reagents used are all of analytical grade.

(2)Characterization of the Catalysts

BET

N_2 adsorption/desorption isotherms of the catalysts were obtained in a Builder SSA-4200 adsorption instrument using N_2 as the adsorbent. The amount of catalysts used was 150mg, prior to the measurement, the samples were out-gassed at 150°C under N_2 flow for 6h, then, the specific surface area, pore volumes and pore sizes were analyzed by N_2 physi-sorption at -200°C, the results were analyzed by the Brunnauer-Emmett-Teller (BET) method.

XRD

The surface phase composition was studied by X-ray diffraction (XRD, D8 advanced) using Cu K α radiation, the tube voltage was 40kV, and the current was 30mA. The samples were scanned over $2\theta=2-80^\circ$ at a ramp rate of 0.06°/s.

CO_2 -TPD

The basicity of the calcined samples was determined by carbon dioxide temperature programmed desorption (CO_2 -TPD) in an AutoChem α 2920 Chemisorption analyzer, approximately 200 mg of each tested samples was placed in the reaction tube, after pretreatment at 450°C for 1h under a He flow of 30ml/min., the sample was cooled to 100°C and then reacted with flowing CO_2 under isothermal conditions and subsequently cooled to room temperature, the CO_2 -TPD was then performed with a ramp of 8°C.min⁻¹. from 100 to 800°C under a He atmosphere.

TEM

The morphology of the catalysts after reduction was determined by transmission electron microscopy (TEM, JEM2010), the samples were mixed with alcohol and deposited on a Cu grid covered with a perforated carbon membrane.

H₂-TPR

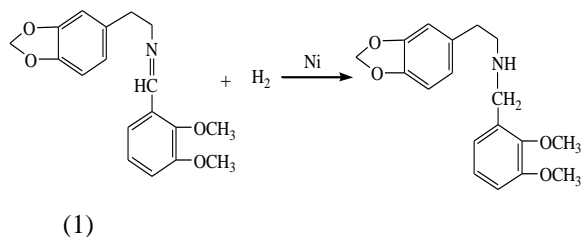
The optimum reduction temperature of the catalysts was determined by temperature programmed reduction of hydrogen (H₂-TPR) in an AutoChemII2920 Chemisorption analyzer, approximately 200 mg of each tested samples was placed in the reaction tube, the temperature was programmed to ramp at 8°C.min⁻¹, to 400°C and hold for 30min under a Helium atmosphere, then the samples was cooled to 100°C, subsequently, the gas line was switched to H₂/Ar, after the baseline was stable, the programmed reduction of H₂ was run from 100°C to 800°C with a heating rate of 8°C.min⁻¹.

XPS

The elemental compositions of the catalyst surface were identified by X-ray Photoelectron Spectrometer (XPS, PHI -5000Versaprobe) equipped with Mg-Kα radiation, the binding energies were referenced to the C1s band at 284.6 eV.

(3) Catalytic Test

The obtained catalysts with different MgO load were used for the hydrogenation of Schiff's base with H₂ to produce precursor of Berberine Hydrochloride using a high-pressure agitated autoclave with 500ml capacity. The autoclave was filled with 0.6g of catalysts and 180ml of absolute methanol containing 125ml of Schiff's base, and was flushed with hydrogen more than three times at room temperature. The reaction were carried out at 85°C-115°C and 1-4MPa hydrogen partial pressure for 2h. the solution was cooled down to room temperature and centrifuged to remove the solid catalysts. The liquid product was collected and the crystal product obtained by crystallization. the reaction formula was shown in (1). the by-products was mainly the substances of raw materials not hydrogenated, and some of N-(2'-hydroxy-3'-methoxy benzyl)-3,4-dioxy-methylene-phenylethylamine inspected by HPLC, from hydrogenation of impurities such as ortho-vanillin in 2,3-Dimethoxybenzaldehyde.



Results and Discussion

BET Results

N₂ adsorption-desorption analysis of the catalysts were conducted using an automated gas sorption analyzer, the surface areas and pore volume were obtained by BET methods, respectively. Table 1 show that the BET surface area, pore volume, and average pore diameter of the catalysts. It can be seen in table1, the 20Ni-6MgO/74Al₂O₃ samples exhibits the highest BET surface area of 61.798m²/g, the largest pore volume of 0.35 cm³/g, and the largest pore diameter of 11.33nm compared to those of Ni/Al₂O₃ and 20Ni-xMgO/(80-x)Al₂O₃ excepted the highest BET surface area of 76.499m²/g of Ni/Al₂O₃, for the average pore diameter, the 20Ni-6MgO/74Al₂O₃ samples were two times as large as Ni/Al₂O₃, it was indicated that the function of expanding role or the mesoporosity was stronger with addition of MgO, and MgO might be regarded as pore-enlarge agent for the bare Al₂O₃ support. An appropriate amount of promoter (MgO 6% load) can enhance the physical properties, however, excessive (MgO 8% load) additives may cause the physical blockage of pores or channels of the catalysts and lead to a lower catalytic activity [3].

Table-1: Physical Properties of the Catalysts Reduced at 500°C.

Catalysts X: MgO wt %	Surface area m ² /g	Pore volumes c m ³ /g	Average pore diameter nm
20Ni/80Al ₂ O ₃	76.499	0.214	5.60
20Ni-2MgO /78Al ₂ O ₃	57.520	0.183	6.38
20Ni-4MgO /76Al ₂ O ₃	56.796	0.204	7.12
20Ni-6MgO /74Al ₂ O ₃	61.798	0.350	11.33
20Ni-8MgO /72Al ₂ O ₃	53.186	0.294	11.07

XRD Results

The XRD patterns of the catalysts with different MgO load were shown in Fig. 1, according to the literature [2, 3, 24], the diffraction peaks at 36.7°,

39.4°, 45.7°, and 66.4° represent Al₂O₃ crystal planes, 36.5°, 43.0°, 62.3°, 74.7°, and 78.6° represent MgO crystal plane, and 37.6°, 43.7°, 63.2°, 75.4°, and 79.4° represent NiO crystal plane. It was reported that NiO could interact with Al₂O₃ at low temperatures (400°C-450°C) to form NiAl₂O₄ spinel oxide, and the amount of aluminate formed increase with the increase of the calcined temperature and time [17]. It observed in Fig. 1a that the diffraction peaks at 37.3°, 44.5° represent the formation of NiAl₂O₄ spinel oxide as a result of interaction NiO precursors species with Al₂O₃ support in the bare Ni/Al₂O₃ catalysts, the diffraction peak at 67.1° represent Al₂O₃ support, and the diffraction peak at 44.5°, 51.8°, and 76.5° represent Ni particles, the Ni particles on the NiAl₂O₄ spinel oxide revealed that only surface reducible NiO on the NiAl₂O₄ spinel oxide was reduced to Ni particles, no obvious NiO diffraction peaks were observed in the the bare Ni/Al₂O₃ catalysts [19]. with the addition of MgO in Fig. 1b-e, the diffraction peak at 37.1° and 43.1° represent the weak construction of MgO-Al₂O₃ solid solution as a result of the weak interaction of MgO with Al₂O₃, the diffraction peaks have a slightly left shift from 37.3° in Fig. 1a to 37.1° in Fig. 1e, and rich of MgO overlapped on the surface of the MgO-Al₂O₃ solid solution with 8 wt% MgO load. The diffraction peak at 44.5° confirmed the NiAl₂O₄ spinel oxide still existed in the catalysts as a result of stronger interaction of NiO with Al₂O₃. Similarly the diffraction peak at 44.5°, 51.8°, and 76.5° represent Ni particles. And the diffraction peak at 62.5° and 67.1° represent bare MgO and Al₂O₃ crystal planes, respectively. The weak diffraction peak at 75.1° and 79.1° represent the formation of the MgNiO₂ as a result of the weak interaction of MgO with NiO [16, 24]. With addition of MgO, the competing interaction had been constructed among MgO, Al₂O₃, and NiO, the weak interaction of Al₂O₃ and NiO with a small number of MgO respectively weakened the stronger interaction of Al₂O₃ with NiO, and more active NiO species were released, it improved the activity of the catalysts. The suddenly decrease of the diffraction peak at 44.5°, 51.8°, and 76.5° and increase at 37.1° and 43.1° in Fig. 1e (8wt% MgO) implied that excessive additives may cause the physical blockage of pores or channels of the catalysts, and lead to a decrease of the reducible NiO species.

TEM Results

The TEM image of the catalysts with different MgO load were shown in Fig. 2, it can be seen clearly that the spinel structure of NiAl₂O₄

existed in the catalysts, and the average diameter of the spinel or the black spinel crystal was about 30-50nm in Fig. 2a, the Ni particles aggregation taken place as a result of the formation of NiAl₂O₄ spinel structure in the Ni/Al₂O₃ catalyst, and the Ni particle only on the surface of the aggregation. With the addition of MgO in Fig. 2b-2e, it can be seen clearly that some MgO-Al₂O₃ solid solution coexisted in the catalysts except the NiAl₂O₄ spinel crystal, the Ni particles more exposed as a result of competing reaction and interaction of MgO with NiO precursors and Al₂O₃ support. the Ni particles and the spinel mix were more uniformly dispersed than others in Fig. 2f, and the average diameter of Ni particles were about 10-20nm.

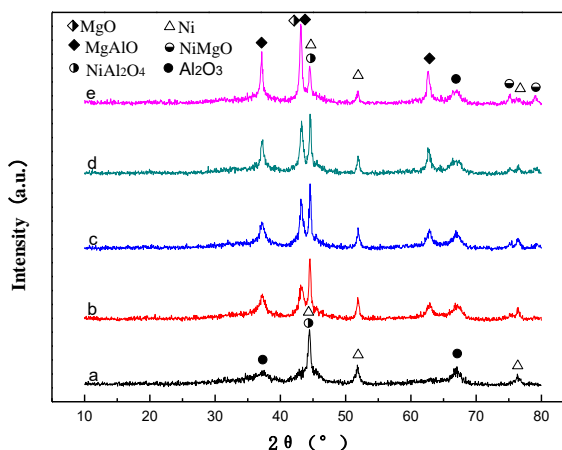


Fig. 1: The XRD patterns of the catalysts with different MgO load.
(20Ni-xMgO/(80-x)Al₂O₃: x, wt%: a=0, b=2, c=4, d=6, e=8)

H₂-TPR

The Fig. 3 present the H₂-TPR profiles of the catalysts with different MgO load, according to the literature [24], the measured reduction temperature of pure NiO was about 340°C., the Ni/Al₂O₃ exhibit a fourth reduction peak from 340°C, to 400°C, 410°C, to 500°C, 500°C, to 650°C, and 650°C, to 800°C, which is assigned to the reduction of Ni²⁺ in the usually classified four types α, β₁, β₂, and γ NiO species interaction with Al₂O₃ support in Fig. 3 a, the peaks located in the low temperature region (340-400) indicated reducible or free nickel oxides species possessing a weak interaction with alumina support. The peak located at the high temperature peaks are assigned stable nickel aluminate phase with the spinel structure NiAl₂O₄. H₂ consumption revealed that the β₁

and β_2 -type NiO are the dominant species in the Ni/Al₂O₃ catalysts. In Fig. 3b, with the addition of 2 wt% MgO, the catalysts exhibit fourth reduction peaks stillly, but the H₂ consumption attribute to β_1 -type NiO was obviously higher than β_2 -type, just not like in the bare Ni/Al₂O₃ catalysts, it revealed that the β_1 -type NiO species expoussed more as a resul of MgO interaction with Al₂O₃ support, and the higher of H₂ consumption peak at 650-800°C which attribute to the coexist of the MgO-Al₂O₃ solid solution and NiAl₂O₄ spnel. With the addition of 4 wt% MgO, the H₂ consumption attribute to α -type NiO increased and the β_1 -type NiO species decreased in Fig. 3b, and the more higher of H₂ consumption peak at 650-800°C, it indicated that the coexist of the NiO-MgO-Al₂O₃ solid

solution or NiMg(Al)O mixed oxide at the NiO-Al₂O₃ interface and a higher interaction between nickel atoms and the neighboring cations. It observed in Fig. 3d that the H₂ consumption peak which attribute to the β_1 -type NiO species was obviously become high and length, but the H₂ consumption peak at 650-800°C, become moderately, and the reduction temperature decreased to 340°C, it revealed that more reducible α and β_1 -type NiO species exposed or overlapping on the support. Further increased the MgO load in Fig. 3e, the change trend taken place just like in Fig. 3c. so the 6 wt% MgO addition confirmed the most reducible nickel species, and so on the most nickel particles and the most small diameter.

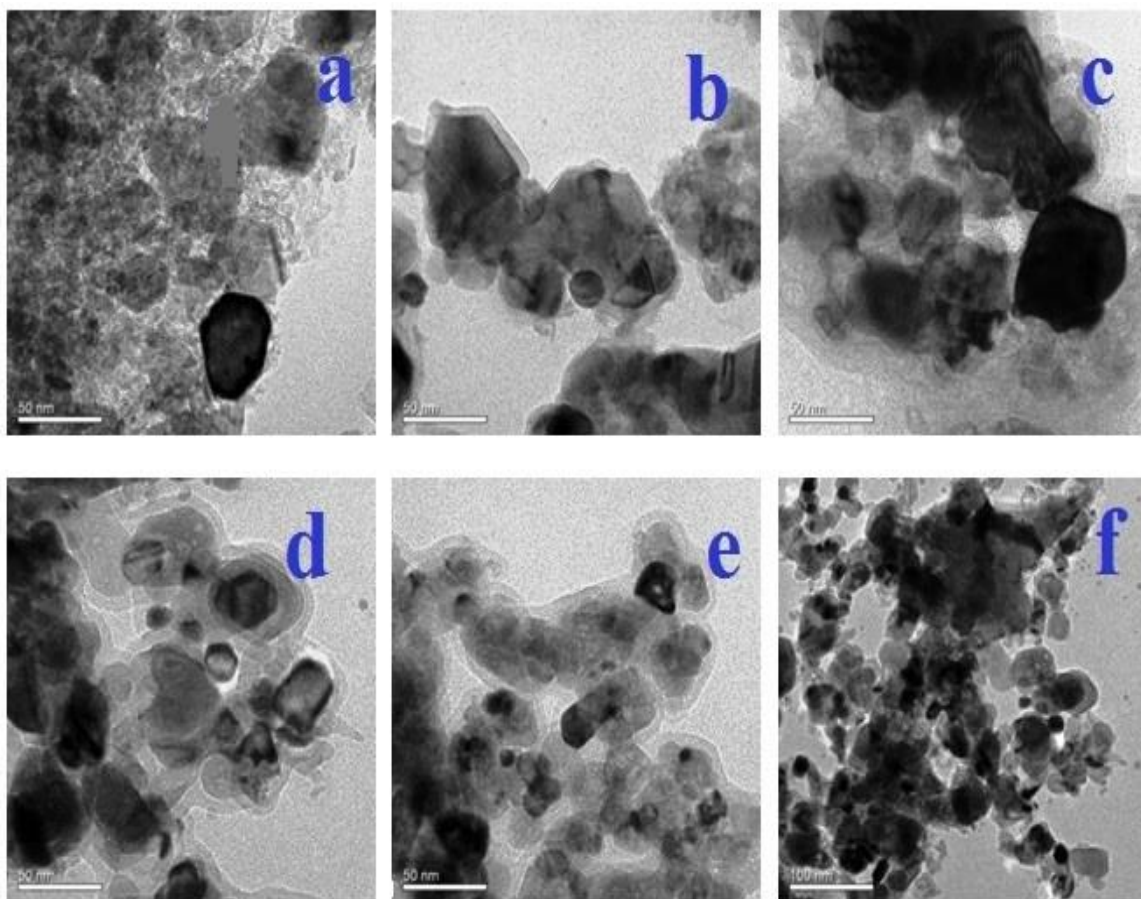


Fig. 2: The TEM image of the catalysts with different MgO load.
(20Ni-xMgO/(80-x)Al₂O₃: x, wt%: a=0, b=2, c=4, d,f=6, e=8)

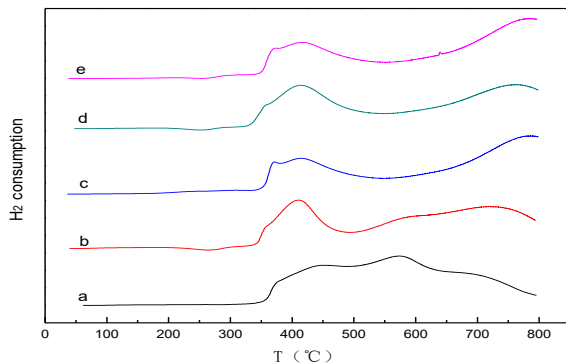


Fig. 3: The H₂-TPR profiles of the catalysts with different MgO load.

(20Ni-xMgO/(80-x)Al₂O₃: x, wt%: a=0, b=2, c=4, d=6, e=8)

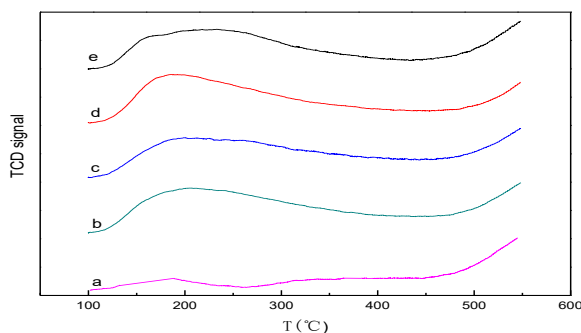


Fig. 4: The CO₂-TPD profiles of the catalysts with different MgO load.

(20Ni-xMgO/(80-x)Al₂O₃: x, wt%: a=0, b=2, c=4, d=6, e=8)

CO₂-TPD

The obtained CO₂-TPD profiles of the catalysts with different MgO load was shown in Fig. 4, the amount of CO₂ desorbing in the different temperature ranges from 100°C, to 275°C, 275°C to 450°C, even more than 450°C in Fig 4a, the results indicated that weak surface basicity exhibited in the catalysts as a results of the presence of no reduction of nickel oxide species (revealed in the H₂-TPR test), the peak at 100°C to 275°C (the LT-peak) corresponding to the desorption of the adsorbed CO₂ on the weak acid sites of the Ni/Al₂O₃ catalysts, the peaks at 275°C to 450°C represents the desorption of the adsorbed CO₂ on the strong basic sites. It was clearly observed that after the addition of MgO (2-8 wt%), the peaks at 100°C to 275°C increased visibly more than at 275°C to 450°C in Fig 4b-e, the results indicated that the magnesium addition decreased the density of Brounded acid sites, but increased the number of Lewis acid sites [33] with addition of 2 wt% MgO, it

can be observed that a suddenly increase of the amount of CO₂ desorbing in the different temperature ranges from 100°C to 275°C, 275°C to 450°C, even more than 450°C in Fig 4b, the stronger surface basicity can be attributed to the coexist of MgO-NiO, or NiMgAlO components in the catalysts. with increase addition to 6 wt% MgO, the content in the catalysts results in a shift of the CO₂ desorption peak to lower temperature, which is indicative of a shift in surface basicity of the catalysts. This suggests that Mg²⁺ in the catalysts contribute to strong basic sites [8], and the difference of surface basicity can be attribute to the changes of Mg/Al ratio. Moreover, CO₂-TPD at high temperature (even more than 450°C) can be attributed to the thermal decomposition of carbonates formed during CO₂ adsorption.

XPS

XPS was used to determine the surface nickel and ion species in the synthesized catalysts samples, the Ni 2p XPS spectra of the catalysts with 6 wt% MgO load was shown in Fig 5, in the Ni 2p spectra, the peaks at around 855.7 and 873.1 eV were attribute to the spin-orbit split lines of Ni 2p_{3/2} and Ni 2p_{1/2}, the characteristic peaks of Ni 2p_{3/2} and Ni 2p_{1/2} were accompanied by shakeup satellites at binding energies of about 861.7 and 880 eV corresponding to charge-transfer transitions. The XPS spectra in the Ni 2p_{2/3} region of the Ni/Al₂O₃ sample can be fitted to two peaks centered at 855.2 and 856.5 eV, attribute to Ni²⁺ present in the octahedral positions of NiAl₂O₄ phase formed by the reaction of NiO and Al₂O₃, respectively. With increase of MgO load, the Ni2p_{3/2} peak of the bimetallic catalysts exhibited a slight blue shift compared with that of Ni/Al₂O₃, indicated that the enhanced electron density of the nickel oxide species due to the addition of MgO to Ni/Al₂O₃.

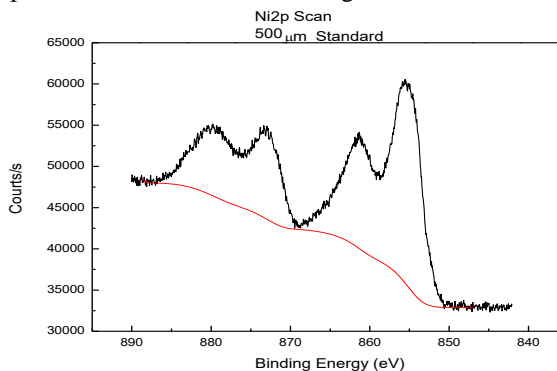


Fig. 5: The XPS spectra of the 20Ni-6MgO/74Al₂O₃ catalysts.

The effects of obtained catalysts with different MgO load were tested, the conversion and the selectivity for the catalytic hydrogenation of N-(2',3'-dimethoxy benzyl)-3,4-dioxy-methylene-phenylethylamine(Shiff's base) were summarized in table2. It can be seen that the 20Ni-6MgO/74Al₂O₃ gave the highest selectivity and yield, this might attributed to the electron-deficient Ni surface favored the adsorption of aromatic ring of Shiff's base as a result of the lateral repulsion of large molecules among adsorption [6], appropriate mesoporosity for large molecules, appropriate surface acidity and basicity of support for Shiff's base and H₂. the pore diameter has regular change with addition0, 2,4,6,8%MgO in table 1, and the reactants was big molecular, the highest pore diameter ,the highest yield, mainly attribute to the highest pore diameter was in favor of the transfer process of big reactants molecular. The surface area and conversion of reaction in table 2 was not regular with the addition of MgO, the surface area was important in absorption of hydrogen during the hydrogenation,not regular change mainly attribute to the impurities such as ortho-vanillin in 2,3-Dimethoxybenzaldehyde.

Table-2: The conversion and selectivity of the reaction with different MgO load.

Catalysts X: MgO wt %	conversion %	selectivity %	Yields %
20Ni/80Al ₂ O ₃	88.50	50.51	44.70
20Ni-2MgO /78Al ₂ O ₃	99.70	90.31	90.04
20Ni-4MgO /76Al ₂ O ₃	95.45	98.55	94.07
20Ni-6MgO /74Al ₂ O ₃	94.87	99.70	94.63
20Ni-8MgO /72Al ₂ O ₃	99.40	90.86	90.31

Conclusions

The modification of the nickel based alumina support catalysts by addition of MgO directly affect the surface composition of the catalysts, with the appropriate amount of promoter MgO (6 wt%), the weak formation of MgO-Al₂O₃ and MgO-NiO solid solution as a result of competing interaction of MgO with Al₂O₃ support and NiO restrained the strong interaction of NiO and Al₂O₃ support, which favored the d particles, and improved the transport of large molecules reactants and products. The improvement of basicity or the decrease in the number of acid centers in the catalysts avoid the secondary reactions , and subsequently resulted in high catalytic activity. the utilization of meso-porous 20Ni-6MgO/74Al₂O₃ for catalytic hydrogenation of N-(2',3'-dimethoxy benzyl)-3,4-dioxy-methylene-phenylethylamine(Shiff's base) with the highest selectivity of 99.70% and yields of 94.36% implied that the instead of Raney Ni

was feasible ispersion of active Ni centers and improved the reducible degree of NiO species on the surface of the catalysts. The mesoporosity exhibited by, such as the highest specific surface area, the largest pore volume and the largest average pore diameter among the modified catalysts, favored the high dispersion of metal Ni.

Acknowledgements

This work was supported by the National Natural Science Foundation of China(No. 51402199, 51422210), and Key Laboratory Project of Education Department of Liaoning Province (No. LZ2015060).

References

1. T. J. Wang, Y. P. Li, C. G. Wang, X. H. Zhang, L. L. Ma and C. Z. Wu. Synthesis Gas Production with NiO-MgO/ γ -Al₂O₃/Cordierite Monolithic Catalysts in a Pilot-Scale Biomass-Gasification-Reforming System. *Energy Fuels*, **25**, 1221 (2011).
2. Y. P. Li, T. J. Wang, C. Z. Wu, Y. Gao, X. H. Zhang, C. G. Wang, M. Y. Ding, L. L. Ma. Effect of Alkali Vapor Exposure on Ni-MgO/ γ -Al₂O₃/Cordierite Monolithic Catalyst for Biomass Fuel Gas Reforming. *Ind. Eng. Chem. Res.*, **49**, 3176 (2010).
3. G. Chen, C. Liu, W.C. Ma, B.B. Yan, N. Ji. Catalytic Cracking of Tar from Biomass Gasification over a HZSM-5-Supported Ni-MgO Catalyst. *Energy Fuels*, **29**, 7696 (2015).
4. Y.J. Wang, T.T. Ji, X.X. Yang, Y.H. Wang. Comparative Study on Steam Reforming of Single- and Multicomponent Model Compounds of Biomass Fermentation for Producing Biohydrogen over Mesoporous Ni/MgO Catalyst. *Energy Fuels*, **30**, 8432(2016).
5. F. Seyedeyn-Azad, J.Abedi, S. Sampouri. Catalytic Steam Reforming of Aqueous Phase of Bio-Oil over Ni-Based Alumina-Supported Catalysts. *Ind. Eng. Chem. Res.*, **53**, 17937(2014).
6. J. Zhao, H. Chen, J. Xu, J.Y. Shen. Effect of Surface Acidic and Basic Properties of the Supported Nickel Catalysts on the Hydrogenation of Pyridine to Piperidine. *J. Phys. Chem. C.*, **117**, 10573(2013).
7. M. C. Abello, M. F. Gomez, L. E. Cadús. Oxidative Dehydrogenation of Propane over Molybdenum Supported on MgO- γ -Al₂O₃. *Ind. Eng. Chem. Res.*, **35**, 2137(1996).
8. Z. Jiang, J.X. Su, M. O. Jones, H.H. Shi,

- T.C.Xiao, P.P. Edwards. Catalytic Partial Oxidation of Methane over Ni-Based Catalysts Derived from Ni-Mg/Al Ternary Hydrotalcites. *Energy Fuels*, **23**, 1634(2009).
9. A. Shamsi, J. J. Spivey. Partial Oxidation of Methane on Ni-MgO Catalysts Supported on Metal Foams. *Ind. Eng. Chem. Res.*, **44**, 7298(2005).
 10. S.B. Wang and G.Q. Lu, Catalytic Activities and Coking Characteristics of Oxides-Supported Ni Catalysts for CH₄ Reforming with Carbon Dioxide, *Energy & Fuels*, **12**, 248(1998).
 11. D.D. He, Y.M. Luo, Y.W. Tao, V. Strezov, P.F. Nelson, and Y.J. Jiang, Promoter Effects of Nickel-Supported Magnesium Oxide Catalysts for the Carbon Dioxide Reforming of Methane, *energy fuels*, **31**, 2353(2017).
 12. V. García, J. J. Fernández, W. Ruíz, F. Mondragón, A. Moreno, Effect of MgO addition on the basicity of Ni/ZrO₂ and on its catalytic activity in carbon dioxide reforming of methane, *Catalysis Communications*, **11**, 240 (2009).
 13. Y.C. Zhao, B.S. Liu, and R. Amin, CO₂ Reforming of CH₄ over MgO-Doped Ni/MAS-24 with Microporous ZSM-5 Structure, *Ind. Eng. Chem. Res.*, **55**, 6931 (2016).
 14. S.B. Wang, G. Q. Lu. A Comprehensive Study on Carbon Dioxide Reforming of Methane over Ni/ γ -Al₂O₃ Catalysts. *Ind. Eng. Chem. Res.*, **38**, 2615 (1999).
 15. L.F. Bobadilla, A. Penkova, F. Romero-Sarria, M.A. Centeno, J.A. Odriozola. Influence of the Acid-Base Properties over NiSn/MgO-Al₂O₃ Catalysts in the Hydrogen Production from Glycerol Steam Reforming. *International Journal of Hydrogen Energy.*, **39**, 5704 (2014).
 16. A. Penkova, L. Bobadilla, S. Ivanova, M.I. Domínguez, F. Romero-Sarria, A.C. Roger, M. A. Centeno, J.A. Odriozola. Hydrogen Production by Methanol Steam Reforming on NiSn/MgO-Al₂O₃ Catalysts: The Role of MgO Addition. *Applied Catalysis A: General.*, **392**, 184 (2011).
 17. M. S. Li, X.D. Wang, S.R. Li, S.P. Wang, X.B. Ma. Hydrogen Production from Ethanol Steam Reforming over Nickel Based Catalyst Derived from Ni/Mg/Al Hydrotalcite-like Compounds. *Int. J. Hydr. Energy.*, **35**, 6699 (2010).
 18. D.H. Mei, V. L.Dagle, R. Xing, K.O. Albrecht, R.A. Dagle. Steam Reforming of Ethylene Glycol over MgAl₂O₄ Supported Rh, Ni, and Co Catalysts. *ACS Catal.*, **6**, 315 (2016).
 19. X.X. Yang, Y.J. Wang, M.W. Li, B.Z. Sun, Y.R. Li, Y.H. Wang. Enhanced Hydrogen Production by Steam Reforming of Acetic Acid over a Ni Catalyst Supported on Mesoporous MgO. *Energy Fuels*, **30**, 2198(2016).
 20. R. Ullah, Z.Q. Zhang, P. Bai, P.P. Wu, D.Z. Han, U. J. Etim, and Z.F. Yan, One-Pot Cation Double Hydrolysis Derived Ni/ZnO-Al₂O₃ Absorbent for Reactive Adsorption Desulfurization, *Ind. Eng. Chem. Res.*, **55**, 3751 (2016).
 21. X.F. Lin, Y.H. Lv, Y.Y. Xi, Y.Y. Qu, D. L. Phillips, C.G. Liu. Hydrogenolysis of Glycerol by the Combined Use of Zeolite and Ni/Al₂O₃ as Catalysts: A Route for Achieving High Selectivity to 1-Propanol. *Energy Fuels*, **28**, 3345 (2014).
 22. W. Gac, A. Denis, T. Borowiecki, L. Kępiński. Methane Decomposition over Ni-MgO-Al₂O₃ Catalysts. *App. Cata. A: Gen.*, **357**, 236 (2009).
 23. Y. X. Li, Y.H. Guo, B. Xue, Catalytic combustion of methane over M(Ni, Co, Cu) supported on ceria-magnesia, *Fuel Processing Technology*, **90**, 652 (2009).
 24. D. C. Hu, J. J. Gao, Y. Ping, L. H. Jia, Poernomo Gunawan, Ziyi Zhong, Guangwen Xu, Fangna Gu, Fabing Su. Enhanced Investigation of CO Methanation over Ni/ Al₂O₃ Catalysts for Synthetic Natural Gas Production. *Ind. Eng. Chem. Res.*, **51**, 4875 (2012).
 25. D. Q. Huang, M. Ke, X. J. Bao, H.Y. Liu. Fe-Promoted Ni/Al₂O₃ Thioetherification Catalysts with Enhanced Low-Temperature Activity for Removing Mercaptans from Liquefied Petroleum Gas. *Ind. Eng. Chem. Res.*, **55**, 1192 (2016).
 26. J.Y. Liu, Catalysis by Supported Single Metal Atoms, *ACS Catalysis*, **7**, 34 (2017).
 27. P. Munnik, P. E. D. Jongh, and K.P. D. Jong, Recent Developments in the Synthesis of Supported Catalysts, *Chemical Reviews*, **115**, 6687 (2015).
 28. M. Ahmadi, H. Mistry, and B. Roldon Cuenya, Tailoring the Catalytic Properties of Metal Nanoparticles via Support Interactions, *Journal of Physical Chemistry Letters*, **7**, 3519 (2016).
 29. H. Tian, X.Y. Li, L. Zeng, and J.L. Gong, Recent Advances on the Design of Group VIII Base-Metal Catalysts with Encapsulated Structure, *ACS Catalysis*, **5**, 4959 (2015).
 30. R. S. Lima, J. S. Moura, G. C. D. Araujo, V. D. O. Mateus, M. O. D. G. Souza, Properties and phase composition of Ni-MgO-La₂O₃ systems submitted to different thermal treatments, *Materials Chemistry and Physics*, **135**, 1084 (2012).
 31. T. Panczyk, W. Gac, M. Panczyk, T. Borowiecki,

- W. Rudzinski. On the Equilibrium Nature of Thermodesorption Processes. TPD-NH₃ Studies of Surface Acidity of Ni/MgO-Al₂O₃ Catalysts. *Langmuir*, **22**, 6613(2006).
32. N. Lopez and F. Illas, Ab Initio Modeling of the Metal-Support Interface: The Interaction of Ni, Pt, and Pt on MgO (100), *J. Phys. Chem. B*, **102**, 1430 (1998).
33. S. W. Lee and S. K. Ihm, Characteristics of Magnesium-Promoted Pt/ZSM-23 Catalyst for the Hydroisomerization of n-Hexadecane, *Ind.Eng.Chem.Res.*,**52**, 15359 (2013).